2022 IEEE/SICE International Symposium on System Integration (SII)
January 9-12, 2022. Narvik, Norway

2022 IEEE/SICE International Symposium on System Integration (SII) | 978-1-6654-4540-5/22/$31.00 ©2022 IEEE | DOI: 10.1109/SII52469.2022.9708778

A telescopic robot arm design performing space-saving motion for autonomous mobile robots

Yusuke Hanafusa[1,2], Hiroki Satoh[2], Yoko Sasaki[2] and Hiroshi Takemura[1,2]

***Abstract*— The paper proposes a compact arm suitable for mounting on a mobile robot that can generate space-saving motions. Standard industrial and collaborative robotic arms are not suitable for mobile robots traveling anywhere in daily life. A robotic arm for mobile robots is required to have the following two compactness requirements. (1) The arm does not interfere with surroundings when it is not in use, such as running. (2) The arm does not interfere with the robot itself or surrounding obstacles while performing a task at a given location. We propose a design of a mobile robot arm with two telescopic links. The proposed arm has mechanisms for compactness, multi-stage expansion and contraction by a lead screw, and folding wires in the telescopic link shells. A primary motion generator is implemented to the proposed arm that moves the arm tip to the specified 3D position. Its' small pass-through volume allows operation in confined spaces. The effectiveness of the proposed compact arm was verified by simulation and the actual prototype arm.**

I. INTRODUCTION

Autonomous mobile robots are now able to move autonomously in a variety of indoor and outdoor daily life spaces. In daily life, robots are required to perform various tasks associated with mobility, such as checking traffic lights and surroundings when crossing a road, pushing elevator buttons, opening and closing doors, and so on. Robot manipulators are used to performing these tasks. Industrial robots and cooperative robots often occupy a large space due to the size of the robot itself and its movements. Therefore, existing robot manipulators are not suitable for autonomous mobile robots that can travel anywhere in our daily living space.

The goal of this study is to produce a compact arm suitable for mounting on a mobile robot. The compactness required to the arm for mobile robots has two meanings; (1) small footprint and fold up small when not in use, such as while driving, (2) Capable of operating without interference in confined areas at arbitrary locations. The proposed arm has compact hardware design using a telescopic mechanism and a small occupied volume operation.

Mashimo et al. proposed a two-link telescopic mechanism using a pantograph mechanism as an arm with extendible joints[1]. It is intended for work in a confined space such as the kitchen of a household robot, and has the advantage of allowing free movement of the elbow joint. Yuan et al. proposed a cable-based multi-stage telescopic mechanism[2]. This mechanism is intended to mount a camera on a mobile surveillance robot and has high elasticity. Li et al. proposed an arm that uses a rigid chain structure for the links of the arm to extend and retract[3][4]. This mechanism allows the unwanted part of the arm to be moved to the most convenient position and is very compact. Luis et al. have produced a sea urchin-like robot that moves using a rigid chain extension mechanism[5]. It can move and adapt in semi-rigid environments, which is not possible with common spherical robots, by stretching and shrinking its spines. Sato and Fukui use a steel belt to achieve a telescopic mechanism with an up-and-down lifting motion[6][7]. The robot was designed to be hung on the ceiling to perform pick-and-place tasks in the living room. Sorioka et al. use a telescopic arm to support a wall climbing robot[8]. The arm is transmitted to the rack and pinion gears via pulleys and drive belts to achieve precise extension and retraction.

As described above, research has been done on telescopic arms and mechanisms themselves. However, these mechanisms interfere with the movement of the robot when it is mounted, and it is difficult to use the mechanism as a link of the arm. The proposed arm has a compact telescopic mechanism that uses lead screws and includes wiring and deflection countermeasures. The compact motion generation is achieved by defining the timing of the extension and retraction of the two links. The compact motion is verified by simulation and the implemented actual prototype arm.

II. MECHANICAL DESIGN

This section proposes the hardware design of the proposed two-link telescopic arm, wiring method, and deflection countermeasures.

A. Overall structure

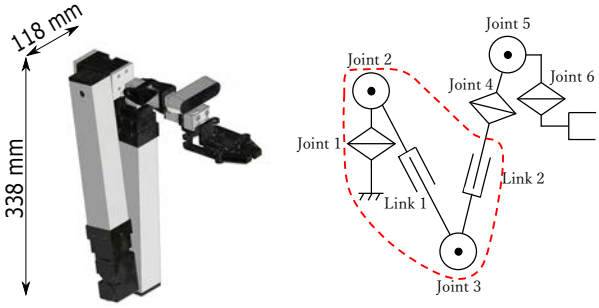

(a) 3D image (b) Mechanism

Fig. 1. Image of the proposed telescopic arm

*This work was supported by the New Energy and Industrial Technology Development Organization (NEDO).

[1]Department of Mechanical Engineering, Tokyo University of Science, 2641 Yamazaki, Noda-shi, Chiba 278-8510, Japan

[2]National Institute of Advanced Industrial Science and Technology, 2-3-26 Aomi, Koto-ku, Tokyo 135-0064, Japan

Fig.1 shows the overall image of the arm including a sample gripper. The proposed arm is based on a PUMA-typed robot with two links that can both be extended and retracted. Fig.1(b) describes a simplified view of the proposed arm. The unit with a linear motion joint is called a telescopic link. The arm consists of 8 degrees of freedom (DOF), 6 joints, and 2 telescopic links. In this paper, the arm body with five DOF is shown by the dotted red frame except for the 4, 5, and 6 joints of the fingers.

Compared with general vertically articulated robots, this arm can be stored in a smaller and more compact space when not in use. In addition, the elbow joint can be positioned relatively freely to avoid obstacles when operating in a narrow space. Compared with the polar-coordinate-type robot, this robot has the flexibility to go around obstacles and has a high hand speed.

B. Telescopic mechanism

As a link structure, we present a three-stage telescopic mechanism using a single actuator. A telescopic mechanism is housed inside the shell to realize a compact arm with multi-stage extension and retraction. A single actuator provides three levels of extension and retraction. It gives a lightweight design and achieves high telescopic performance.

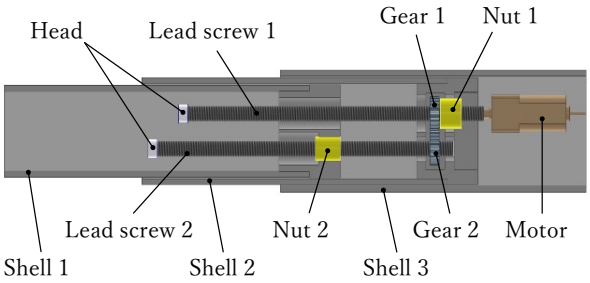

Fig. 2. The multi-stage telescopic mechanism using lead screws

Fig.2 shows the link structure. The telescopic mechanism has a three-stage nested shell and consists of a lead screw, a gear, and a nut. The lead screw 1 connected to the drive motor rotates, and nut 1 and shell 2, which are connected axially, move linearly. When nut 1 moves to the head of the lead screw, nut 1 and gear 1 rotate, and the power is transmitted to the fixed gear 2 and the lead screw 2. The rotation of the lead screw 2 causes shell 3, which is connected to nut 2, to move linearly.

C. Guide structure for expansion and contraction

There is a gap between the nested shells in order to eliminate friction caused by the fitting. However, the gap causes the whole arm to deflect and sway. To solve the problem, bearings are attached to all link shells. This structure provides high rigidity in spite of the multi-stage telescopic mechanism.

The guide structure of the shells is shown in Fig.3.The shells are made of square rectangular pipes. The nested shells should be arranged so that the bearings (shown in orange) touch on the inside and outside. By placing the bearings at the corners of the four planes, distortion in the tube axial direction is reduced. In addition, fixing the bearings at the ends of the shells is expected to enhance the elasticity. This structure enables smooth extension and retraction of the arm.

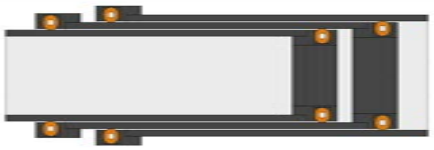

Fig. 3. Guide structure of the link shells

D. Wiring structure in the shell

The arm contains wires for actuators and sensors. These wires are stored inside the link not to become entangled when the link is extended or retracted. The space inside the link is limited due to the extension and retraction mechanism.

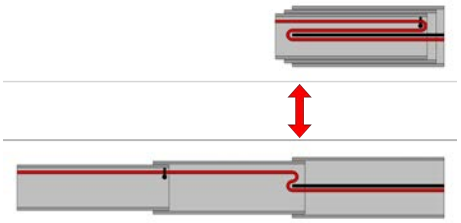

Fig. 4. Wiring structure in the shell

As a wiring structure for the proposed arm, we propose the cable folding design inside the link as the arm is extended or retracted. FFC (Flexible Flat Cable) is applied for wiring. Fig.4 shows a cross-sectional view of the cable folding structure. The red line indicates the FFC. It is folded along the flat bar (shown in black) fixed to shell 3 (outermost shell). A retainer (shown in black) fixed at the root of shell 1 is used to reproduce the folding. It has a space-saving structure that automatically folds up as it expands and contracts.

III. MOTION CONTROL

This section proposes the compact motion generation of the proposed arm. The function of the basic motion is to control the hand tip position to the specified three-dimensional position with respect to the root of the arm. In this section, we assume that the arm can operate in a confined space, and generate motions including collision avoidance with the robot itself and surrounding objects.

A. Path planning

In the implementation of motion generation, we aim for compact motion. This arm, which has five degrees of freedom up to the end of the hand, has more degrees of freedom in the link structure than in the workspace. Therefore, the posture

of the arm is determined by giving each joint a purpose of the motion.

First, the artificial potential method[9] is used to generate the hand trajectory. In this method, a virtual potential field is formed in space, and the robot is moved along the gradient direction of the potential field to reach the target position. In this paper, U_o in Eq.(1) and U_d in Eq.(2) are defined as potential functions due to the positional relationship between the obstacle and the target, respectively. U in Eq.(3) is defined as the potential field at the current location of the minion. Eq.(4) represents the gradient of the potential field in Eq.(3).

$$U_o(x,y,z) = \frac{1}{\sqrt{(x-x_o)^2+(y-y_o)^2+(z-z_o)^2}} \quad (1)$$

$$U_g(x,y,z) = -\frac{1}{\sqrt{(x-x_g)^2+(y-y_g)^2+(z-z_g)^2}} \quad (2)$$

$$U(x,y,z) = \sum(w_o U_o + w_g U_g) \quad (3)$$

$$-gradU(x,y,z) = -\left[\frac{\partial U}{\partial x}, \frac{\partial U}{\partial y}, \frac{\partial U}{\partial z}\right] \quad (4)$$

(x,y,z) is the hand position, (x_o,y_o,z_o) is the obstacle position, and (x_g,y_g,z_g) is the target position. w_o and w_g are the weights on the functions for the obstacle and the target, respectively. The displacement of each joint is calculated for each coordinate on the hand trajectory obtained by this method.

B. Small path-through volume motion

In order for this arm to have a small convex-hull, we need to consider the timing of the following two actions. (1) To move only the joints of the arm. (2) To extend and retract the telescopic link. If the joint is rotated after the telescopic link is extended, the sweep-volume becomes large and the motion is not compact. The ideal sequence is to deploy the elbow joint and then extend the elastic link.

Inverse kinematics is performed on the trajectory $\boldsymbol{P}(\boldsymbol{p}_0,\cdots,\boldsymbol{p}_i,\cdots,\boldsymbol{p}_n)$ of the hand obtained by the potential method. If one link of the arm interferes with an obstacle during the process, the first link is telescoped to avoid the obstacle by changing the elbow position. In addition, when the robot can reach the target by moving only the telescopic link, the robot can make a compact motion by moving only the telescopic link. In this case, the elbow position, the hand position ,and the target position are aligned and the second link can be extended.

The above algorithm is shown in the flowchart Fig.5. In the case of 3D motion generation, the base joint can be rotated and swiveled while the arm is folded, which enables motion generation without the bulkiness and simplifies 2D motion generation.

IV. BASIC MOTION EXPERIMENT

This section evaluates the space-saving motion of the proposed telescopic arm designed for autonomous mobile robots. We implemented the proposed arm as a prototype and verified its basic motion on a wheelchair-based robot.

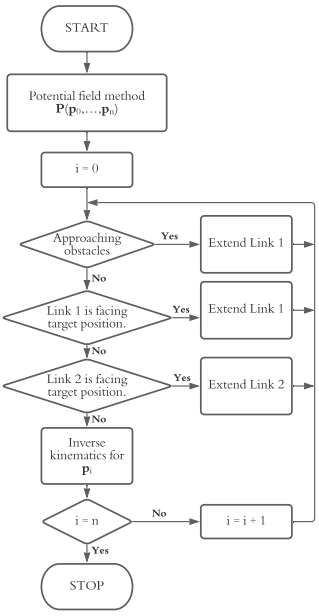

Fig. 5. Flowchart of the algorithm for motion generation

A. Space-saving Motion Evaluation

Verification of motion and compactness using the space-saving motion described in Section III is performed. First, we discuss the definition of compactness. In this paper, compactness is defined by the following two indices. (1) Exclusive area of the arm (2) Volume of Convex-Hull with arm in motion

This subsection is devoted to the verification of the space-saving motion described in Section III. The coordinates of the target are fixed at $y = 0.0$ mm, $z = 270.0$ mm ,and changed to $x = 40.0, 70.0$mm, where the target position is set as near or far. The obstacle is a wall 250 mm high and 250 mm away from the arm base in the x-direction. Simulations are performed with and without the obstacle at the near and far target positions, respectively. The results of the operation using the motion generation method described in Section III under the above conditions are shown in the respective left figures of Fig.6. The green line represents the trajectory of the elbow joint, and the blue line represents the trajectory of the fingertips. The black lines indicate the two links of the arm, and the red surfaces are obstacles. This verification confirms that the pawns reach the target position in all conditions. In free space, the system basically works with minimal links. If it is difficult to reach with the minimum link, the link is extended after deployment at the joint. In situations where it is necessary to avoid obstacles, the arm changes the position of the elbow by extending the first link. By extending the second link from that elbow position, the arm reaches the target position.

Next, the compactness is evaluated from the operation results. All the vertices of the link resulting from the movement of the whole arm are the target points of Convex-Hull. Then, the volume of the obtained solid is calculated. In this paper,

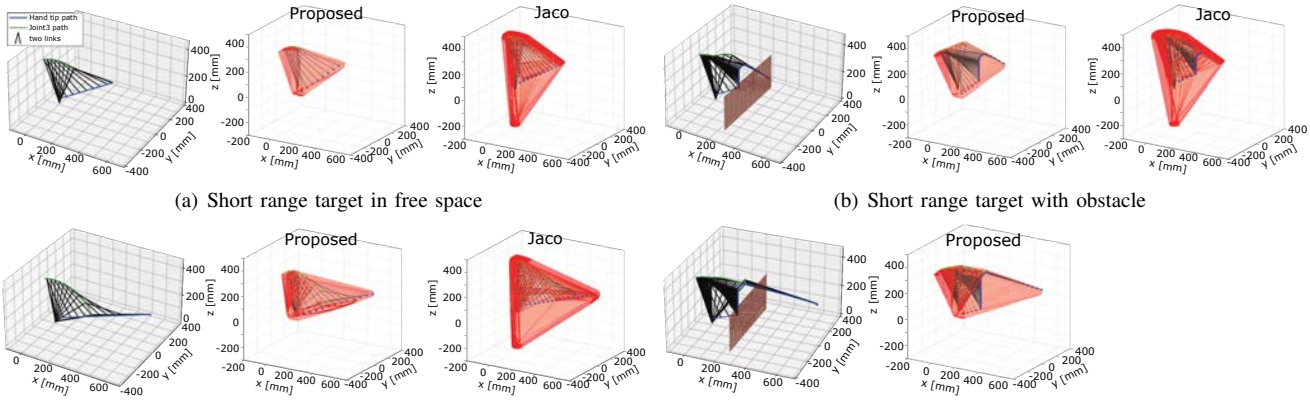

(a) Short range target in free space

(b) Short range target with obstacle

(c) Long distance target in free space

(d) Long distance target with obstacle

Fig. 6. Simulation results of the arm passing volume evaluation

Jaco gen2[1] is used as a general non-stretchable arm and compared with the stretchable arm. The lengths of the two links of Jaco are 410 mm and 344 mm from the root. The Convex-Hull volumes of the two arms are shown in the center and right panels of Fig.6. The farther the target position is, the larger the solid appears to be, and it also appears larger when there is an obstacle. It can be seen that more space was needed to avoid the obstacle. In addition, when there is an obstacle and the target position is far away, the proposed arm can reach the place where the existing arm cannot reach. A comparison of the calculated volumes is shown in Table I. In each situation, the volume of the arm is about two times

TABLE I

CONVEX HULL VOLUME OF EACH MOTION

	Free space		Obstacle installation	
	Near	Distant	Near	Distant [cm^3]
Proposed	8,062	11,685	9,758	15,324
Jaco gen2	18,559	27,476	19,437	-

smaller than that of the existing arm, and it can be said to be compact. When the target position is close, we do not stretch it and use the smallest link to reach it. In a distant situation, the sweep-volume is reduced by extending the link after the joint is deployed.

B. Prototype Implementation

Fig. 8 shows the implemented prototype arm equipped with a wheelchair-based robot[2]. The arm is placed at the front right. When folded, it does not protrude from the wheelchair and its small footprint does not interfere with mobility (Fig.7(a)). The expanded view is shown in Fig.7(b). The proposed arm can be extended by 600 mm in total, with a maximum reach of 1190 mm. In the following evaluation, the axis origin is the root of the arm, the front direction is the positive X-axis and upward is the positive Z-axis.

The hardware specification is summarized in Table II. The telescopic linkages use aluminum and carbon square

[1]https://www.kinovarobotics.com/en

[2]https://whill.inc/

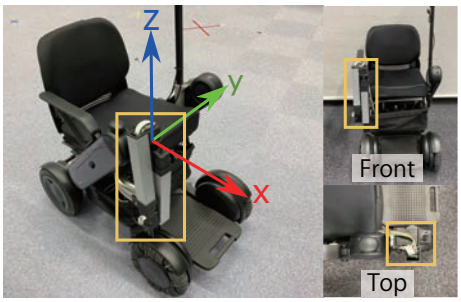

(a) Robot with the proposed arm

(b) Expanded view

Fig. 7. Views of the arm on the robot

TABLE II

SPECIFICATIONS OF THE PROTOTYPE TELESCOPIC ARM

Folded size WxDxH	118×296×338 mm
Weight	1.79 kg
Joint actuators	Dynamixel XM540-W270-R
Telescopic actuators	Pololu 30:1 Micro Metal Gearmotor HPCB
Maximum reach	1190 mm
Link 1 length	310–610 mm
Link 2 length	280–580 mm

pipes, and the actuators are Dynamixel motors. In the motion generation experiment, the calculations and controlling of the trajectory are conducted using a Jetson TX2 module.

Fig. 8 is an application example in a elevator. The compactness of the proposed arm works well in such a small space. The short links prevent large Joint 3 movements and

achieve button pressing action with a small passage volume. Two figures of (a), (b) show the different postures depending on the initial position of Joint 3 (upward or downward). Both can reach the same target in a space-saving manner. A typical two-link arm either overhangs the user's seat or cannot be moved depending on the initial posture.

(a) Joint 3 upward (b) Joint 3 downward

Fig. 8. Example of button pressing action in a narrow elevator

C. Motion Evaluation on the Prototype Arm

We conducted a motion experiment using the telescopic arm that we produced. We evaluated the behavior under two conditions: free space and obstacle avoidance. In this experiment, the hand tip moves from an arbitrary initial posture of the arm to a specified 3D position. The Euclid distance between the target and arm tip positions was measured.

First, we conducted the experiment in free space without any obstacles. The set target coordinates are shown in the Fig. 9. Three points were set in each of the four regions: front, front-left and right, and rear-right, which do not interfere with the robot. Detailed target coordinates are shown in the results (Fig. 11 horizontal axis). The initial posture of the arm is Joint 3 (elbow) up, and the initial position coordinate of the hand tip is $(x, y, z) = (100, 0, 100)$mm.

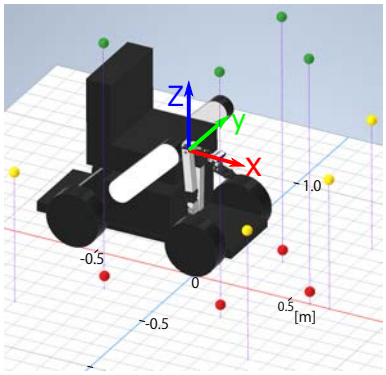

Fig. 9. Experiment setting: goal positions of the free-space experiment

Fig. 10 shows the time series of the arm motion when the target position is at $(x, y, z) = (300, -300, 600)$mm (Yellow marker on the right front of the robot in Fig. 9). First, the robot pointed the arm tip at the target position and then reaches straight for the target. There is no unnecessary overhang of joints and links, and the motion achieved a small passing volume.

The Euclidean distance of the reached arm tip position relative to the 3D target is summarized in Fig. 11. Each

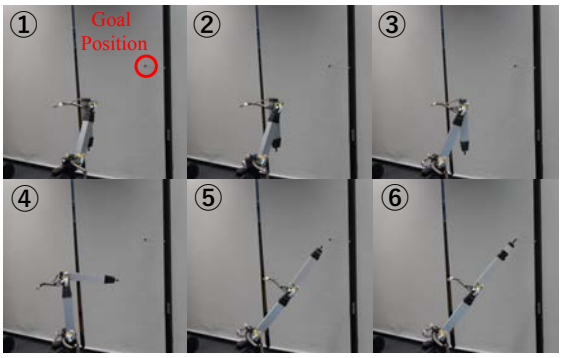

Fig. 10. Operating in free space

point of the three colors represents the average value of 10 trials each. The maximum and minimum values are indicated by error bars. Overall, the results show slight variance. It achieved a highly reproducible operation with a bit of rattle. When compared by direction, the error in the backward direction is more significant than that in the forward direction. It is due to the arm being mounted at a slight backward angle. The error is larger in the upper part than in the lower part when compared for each region. The deflection at the joint attachment point caused it; it was larger when the arm was raised. Although there are differences in the errors due to the joints and attachment points, slight variance for each target indicates sufficient synthesis in the telescopic link.

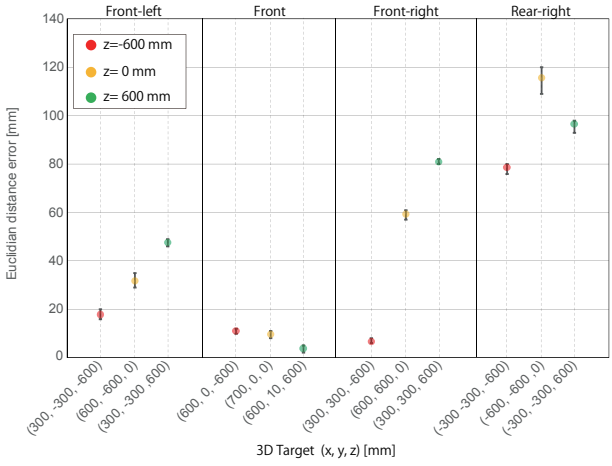

Fig. 11. Euclidean distance error of the reached arm tip

Next, we conducted a motion experiment in a space with an obstacle. The set target coordinates are illustrated in the Fig. 12. We set four targets at the front, forward down-left and right, and left and down. Red markers indicate the target. For each target, two obstacle conditions are tested. Yellow and Green walls indicate the two obstacle conditions. The position of the obstacle was given in advance for motion generation. For all eight conditions (Four targets, two obstacle conditions), we conducted ten trials of motion experiment. The initial position coordinate of the hand tip is $(x, y, z) = (100, 0, 100)$mm.

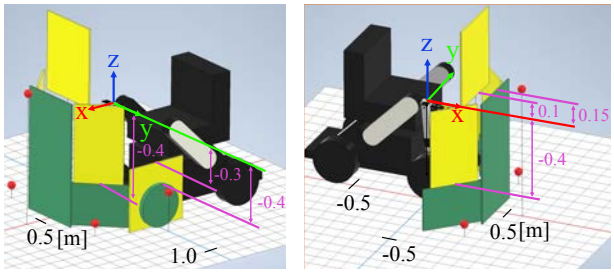

(a) Left front view (b) Right front view

Fig. 12. 3D target and obstacles setting for obstacle avoidance evaluation

Fig.13 shows the time series of the arm motion when the target position is $(x, y, z) = (600, 0, 200)$mm. As an obstacle, a wall was placed parallel to the y-axis at $x = 430$mm. Its upper edge is $z = 150$mm. First, the robot lifts link 2 to avoid the wall, extends link 1, and moves its arm tip to the target. The arm did not extend backward or upward; the generated avoiding motion can minimize its passing volume.

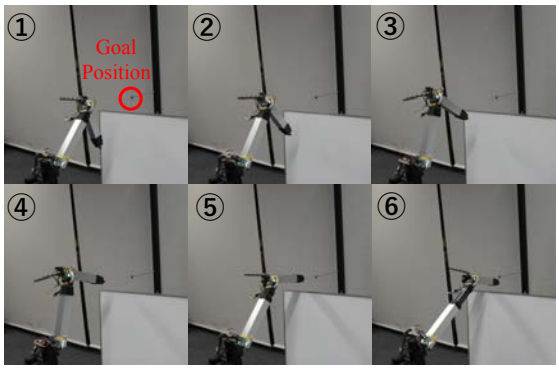

Fig. 13. Obstacle avoidance

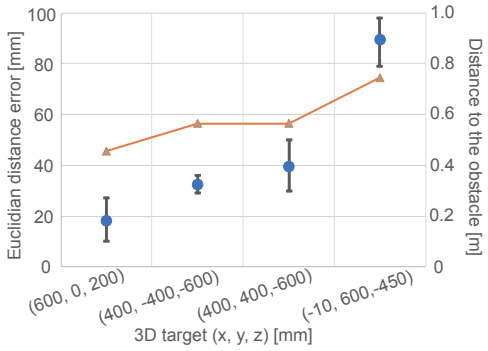

Fig. 14. Euclidean distance error of the reached arm tip

Fig. 14 shows the hand tip position error from the target. The blue dot is the average error, with the error bar indicating the maximum and minimum error. The orange line is the horizontal distance from the arm's origin to the obstacle. These values vary with the same trend, i.e., the farther the obstacle, the larger the error. An installation problem at the base of the arm causes it, and the longer Link 1 was extended, the more the base rattled. For every four targets, the repeatability error is less than 10 mm for each target, even under different obstacle conditions. The error did not change even when the arm posture changed, indicating the high rigidity of the proposed telescopic mechanism.

V. CONCLUSION

This paper proposes a compact telescopic arm design for use with mobile robots. We defined the required compactness for mobile robots, small footprint and volume when folded, and space-saving motion. The proposed arm is based on two links of the multi-stage telescopic links with three joints. It achieved a minimal footprint of about 150cm^2 and 1.19m reach length. The multi-stage telescopic mechanism with a single actuator gives small and lightweight hardware. The two telescopic links allowed for a high degree of freedom in elbow position. The space-saving motion was implemented to the prototype arm. The design of the operation sequence gives a small passing volume motion.

This paper verified the design concept and its basic operation. Future work is required to do actual tasks include feedback such as button pressing and grasping, which integrate the fingers and sensors. As shown in fig.1(a), the system will be equipped with a fingertip and a camera to provide feedback, aiming at accurate fingertip position and posture. Then, more flexible tasks will be possible by generating motions in conjunction with the robots' movement.

REFERENCES

[1] T. Mashimo, R. Diankov, T. Urakubo, and T. Kanade, "Analysis of task feasibility for a home robot using prismatic joints," in *2010 IEEE/RSJ International Conference on Intelligent Robots and Systems*, 2010, pp. 2370–2376.

[2] J. Yuan, W. Wan, K. Chen, Q. Fang, and W. Zhang, "Design and prototyping a cable-driven multi-stage telescopic arm for mobile surveillance robots," in *2014 IEEE International Conference on Robotics and Biomimetics (ROBIO 2014)*, 2014, pp. 1845–1850.

[3] J. Li, R. Liu, L. Zhang, S. Zuo, and H. Wang, "Configuration synthesis and design of a telescopic service robot," in *2018 International Conference on Virtual Reality and Intelligent Systems (ICVRIS)*, 2018, pp. 442–445.

[4] Z. Leiyu, L. Ruifeng, L. Jianfeng, W. Haidong, and Z. Shiping, "Design and dynamic analysis of a telescopic service robot," in *2018 International Conference on Engineering Simulation and Intelligent Control (ESAIC)*, 2018, pp. 121–125.

[5] L. A. Mateos, "Bionic sea urchin robot with foldable telescopic actuator," in *2020 IEEE/ASME International Conference on Advanced Intelligent Mechatronics (AIM)*, 2020, pp. 1063–1068.

[6] T. Sato, R. Fukui, H. Morishita, and T. Mori, "Construction of ceiling adsorbed mobile robots platform utilizing permanent magnet inductive traction method," in *2004 IEEE/RSJ International Conference on Intelligent Robots and Systems (IROS) (IEEE Cat. No.04CH37566)*, vol. 1, 2004, pp. 552–558 vol.1.

[7] R. Fukui, T. Mori, and T. Sato, "Measurement and control scheme for a container transfer robot in living space," in *2009 IEEE/ASME International Conference on Advanced Intelligent Mechatronics*, 2009, pp. 295–301.

[8] Y. Sorioka, T. Yamaguchi, and S. Hashimoto, "Development of a telescopic-arm type, climbing support robot," in *2008 IEEE International Conference on Robotics and Biomimetics*, 2009, pp. 1818–1823.

[9] J.-H. Chuang and N. Ahuja, "An analytically tractable potential field model of free space and its application in obstacle avoidance," *IEEE Transactions on Systems, Man, and Cybernetics, Part B (Cybernetics)*, vol. 28, no. 5, pp. 729–736, 1998.